

Miniature Coherent Velocimeter and Altimeter (MCVA) for Terminal Descent Control on Lunar and Planetary Landers.

Dan Chang (dhc@jpl.nasa.gov), Greg Cardell, Piotr Szwaykowski, Syed T. Shaffat, Patrick Meras
Jet Propulsion Laboratory, 4800 Oak Grove Drive, Pasadena, CA 91109, USA

1 Introduction

While the overall architecture of an Entry Descent and Landing (EDL) system may vary depending on specific mission requirements, measurement of the rate vector with respect to the surface is a primary requirement for the Terminal Descent Control (TDC) phase of any controlled lander.¹ In sharp contrast to the situation with inertial sensors, existing TDC velocimetry solutions— radar and imaging cameras— demand significant compromises among the key traits of accuracy, resource footprint, measurement robustness, and measurement availability. Passive image-correlation sensors suffer from sensitivity to lighting conditions and do not provide a 3-axis rate measurement directly. Doppler radars require either large antenna aperture (difficult to integrate onto lander) or large beamwidths (sensitivity to terrain slope²)

A sensor addressing these shortcomings while delivering cm/s-class velocimetry is sorely needed for future lander missions. Moreover, significant reductions in landing-strut mass can be achieved with touchdown horizontal velocities of less than 10 cm/s for typical lander sizes under consideration. Concurrently, the state-of-the-art for integrated optic components has advanced to the point of making a Doppler lidar ideal for meeting TDC sensing requirements. These are the motivations behind the Miniature Coherent Velocimeter and Altimeter (MCVA), currently being developed under NASA’s Mars Technology Program.

Figure 1 shows the basic MCVA sensor suite, consisting of three or more identical heads. The Doppler shift measured at each yields the component of the velocity vector along that line of sight. A minimum of three heads, mounted along arbitrary but non-degenerate axes, provides the total velocity vector. In addition to the Doppler measurement, a PN-sequence encoded with a Binary Frequency-Shift-Key (BFSK) modulation scheme is used to provide ranging (altimetry). Any

¹It has become unexpectedly important even in air-bag landers. The Mars Exploration Rover (MER) mission fielded— at the last minute— an image-correlation sensor (“DIMES”) to compensate for the local wind using a single directed thruster firing, seconds before cutting the bridle between the lander and its parachute, to achieve acceptable airbag impact loads.

²For example, the Mars Polar Lander radar, with 4-by-5 inch patch antennae, sported roughly 50° beamwidths, forcing the use of a fragile range-gating compensation scheme to isolate the Doppler signal from beam-center.

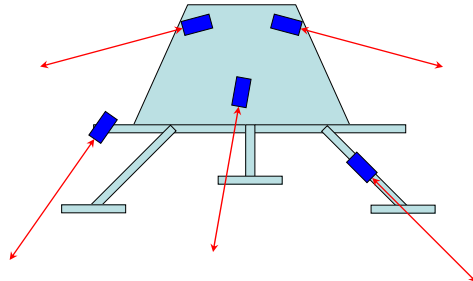


Figure 1: Our terminal descent sensor suite is composed of a minimum of three identical, narrow-FOV heads, arranged at non-degenerate but otherwise arbitrary bore-sights. The flexibility of having small, independent sensors is evident in the ease with which additional axes may be included to, for example, handle large parachute swing angles— a straightforward solution that would be difficult to implement with, say, large radar antennae.

one of the heads can serve as the altimeter channel, although in practice the most nadir-pointing axis is the likely choice.

The key requirements we have set for ourselves are: rate accuracy (per axis) < 10cm/s, range accuracy (per axis) < 10m, altitude range (per axis) 1m - 5km, maximum measurable rate (per axis) 150-200 m/s, data update rate 10 – 100Hz, and mass (per axis) 0.5-1Kg. A sensor with these characteristics would prove useful for all planned Mars and lunar surface missions.

2 Transceiver Design

Figure 2 shows a block diagram of the MCVA sensor. The source is a CW Er³⁺-doped fiber laser with roughly 100mW output, operating in the erbium gain band near $\lambda = 1.54\mu\text{m}$. For this wavelength, 1 cm/s corresponds to a Doppler shift of 13kHz. All optical components are fiber coupled with fused polarization-maintaining fiber interconnects, and fabricated on a single board.

To resolve signed velocities, a Doppler bias is applied to the outgoing beam. Since minimizing MCVA’s power consumption is a key goal, a waveguide LiNbO₃ electro-optic phase modulator with a low $v_{\pi} < 6\text{v}$ is used for generating the bias. When used with a high impedance drive, the current draw is minimal, certainly much lower than the acousto-optic modulators typically used for this purpose. Serrodyne modulation[1] pro-

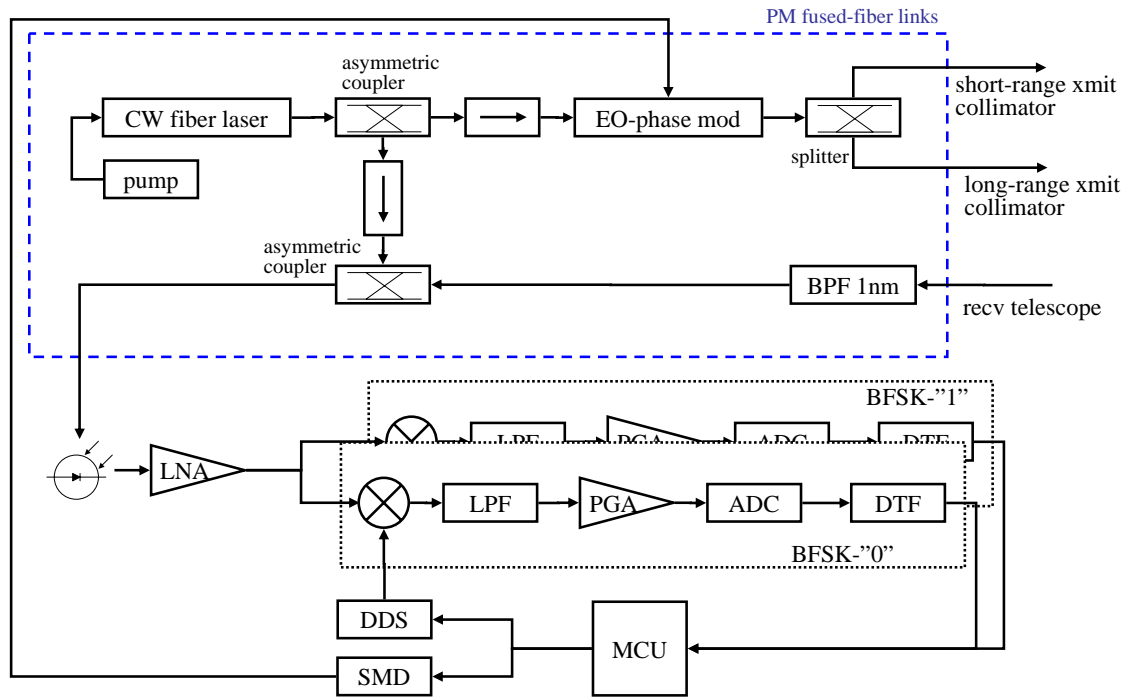


Figure 2: Block diagram of a single MCVA sensor head. All components are fiber coupled and joined by fused PM fiber links. Tracking of the Doppler shift and FM modulation of the PN range code is performed using serrodyne modulation on an LiNbO₃ waveguide electro-optic phase modulator. To achieve the required Tx/Rx isolation, separate transmit and receive telescopes are used, with separate short and long range transmit channels (see text). BPF="band-pass filter," LNA="low noise amplifier," LPF="low-pass filter," PGA="programmable gain amplifier," ADC="A/D converter," DTF="digital tracking filters," BFSK="binary frequency shift keying," MCU="micro-controller unit," DDS="direct-digital synthesizer," SMD="serrodyne modulator."

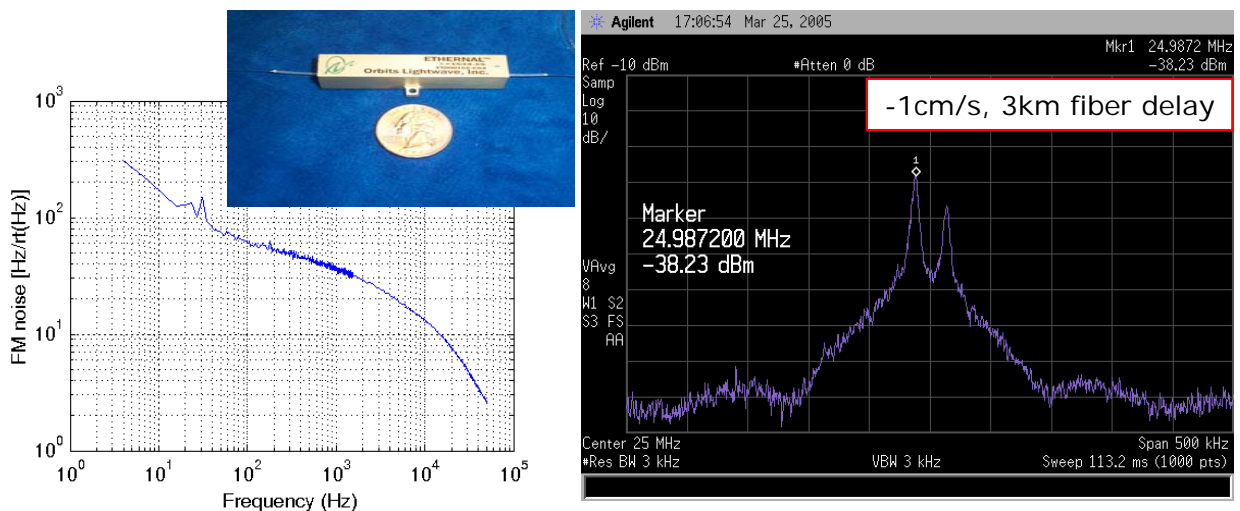


Figure 3: FM-noise performance of fiber laser from Orbits Lightwave Inc. of Pasadena, and a Doppler-shift resolvability test. The attenuated second-peak results from the "imperfect serrodyne modulation" technique described in the text. For reference, 30km corresponds to 10kHz, and a 1cm/s Doppler shift at 1.55 μ m is 13kHz.

vides the frequency shift from the phase modulator. It should be noted that for this application, the serrodyne waveform (ideally a perfect sawtooth— very difficult to generate at several hundred MHz) need only be good enough to allow the receiver to distinguish between sidebands. We therefore synthesize only enough harmonics to achieve a roughly 10dB sideband power ratio, permitting a very efficient quasi-digital implementation of a serrodyne-waveform generator in an Field Programmable Gate Array (FPGA).

The machinery for imposing the Doppler bias can also be used to modulate a pseudo-random noise (PN) code for the altimetry function. The use of amplitude-modulated PN codes for ranging with CW-lidars is a well-established idea.[2] Our implementation— choosing two separate modulation frequencies to encode “0” and “1”— makes MCVA effectively an optical BFSK transceiver.

The transceiver electronics is essentially a specialized heterodyne spectrum analyzer. A single measurement cycle (10-100ms) proceeds as follows. Initially, modulation frequency f_0 corresponding to “0” is selected. The return signal, mixed with the LO beam, generates a beat at f_0 plus the Doppler shift on the photodetector, which is amplified and mixed with the RF local-oscillator signal. The RF-LO range for this application is several hundred MHz, ideal for implementation with Direct Digital Synthesis (DDS) chipsets. The Intermediate Frequency (IF) signal thus generated is filtered, level adjusted, and digitized before being fed into a bank of five narrow-band Digital Tracking Filters (DTF), implemented as Finite Impulse Response (FIR) difference equations on an FPGA (in this case acting as a specialized digital signal processor chip). Our current design IF is 100kHz, and the tracking filters have 1-2kHz bandpasses, covering an aggregate span of about 10kHz. Successful acquisition and tracking, therefore, is defined as the DDS generating an RF-LO which brings the Doppler-shifted f_0 into the span of the tracking filters.

The firmware in the Microcontroller Unit (MCU) adjusts the DDS to re-center the IF signal in the first part of the measurement cycle, thereby producing the velocity measurement. It simultaneously adjusts the parallel DDS shown in Figure 2 such that f_1 is Doppler-corrected as well. In the second part of the measurement cycle, the optical return signal has been frequency modulated with a PN-code sequence, the detection of which using the “BFSK-0” and “BFSK-1” legs of the signal chain is implemented as firmware in the MCU.

The required stability and Q of the tracking filters are what dictated a digital implementation. In addition, the bandwidth and response-time of these filters set respectively the SNR and BFSK-bit rate of the transceiver. The two are in conflict— long range (ie. better SNR) demands narrow bandwidth, while good ranging accuracy (ie. fast PN-code rate) demands wider

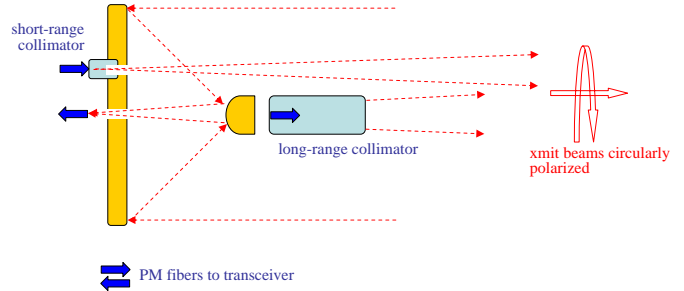


Figure 4: Schematic of MCVA’s telescope design, using two refractive collimators of $\approx F/2$ and a 5cm reflective telescope of $\approx F/1$. Input and outputs are fiber coupled with linear polarization, transformed to circular for free-space propagation.

bandwidth. A digital filter implementation, therefore, is also advantageous in that DTF bandwidths can be adjusted dynamically depending on the part of the measurement cycle. However, this tradeoff is clearly a limitation of the PN-BFSK ranging scheme described here. A characteristic common to all EDL-TDC designs is that range accuracy requirements are most stringent near the surface, when SNR is good. For example: the planned Mars Science Laboratory (MSL) lander requires 10m accuracy for altitudes above 1km, 1m accuracy from 100-1000m, and 10cm accuracy from 4-100m. If the BFSK-PN scheme cannot achieve the required close-in accuracy, a direct and simple fix is to incorporate an AM-PN channel— using a low-power, directly modulated laser diode with a small collimator— to augment that specific part of the entire operating envelope, relegating BFSK-PN to the longer-range altimetry function.

3 Laser

A laser with sufficient coherence to observe kHz-level Doppler shifts at tens of kilometers (for reference- a 0.1ms delay corresponds to a 15km round trip) is the heart of the transceiver. Other equally important requirements are compactness and intrinsic robustness, optical power output, and efficiency. In our development work we are using a 980nm diode-pumped, erbium-doped fiber laser from Orbits Lightwave of Pasadena, CA. As shown in Figure 3, the FM-noise performance exceeds our requirements by a good margin. The FM noise data on the left is provided by the vendor, and is consistent with more ad-hoc measurements conducted with a prototype transceiver in the lab. The figure on right shows the spectrum of a transceiver moved at 1cm/s on a precision track, with 3km of propagation delay simulated by optical fiber. The peak is easily resolvable with a 3kHz resolution-bandwidth, larger than the 1kHz of our tracking filters. (The smaller peak is the signature of the “imperfect serrodyne modulation”

employed, as described above.)

A fiber laser has obvious advantages in compactness and intrinsic robustness. In addition, the Orbits laser has enough margin on spectral purity to allow post-amplification using extra-cavity doped erbium fiber, yielding optical power margin with minimal complication. The fiber laser’s primary weakness is sensitivity to vibration, which at present needs further improvement. Alternatives we have considered are Non-Planar Optical Ring Oscillator (NPRO) Nd:YAG lasers operating at 1319nm, and actively-stabilized semiconductor lasers. Post-amplification is difficult for the former, while the linewidth requirement is pushing the state-of-the-art for the latter

4 Telescope Design

Transmit/receive isolation is a perpetual difficulty with CW-lidar, for which no time-gating can be used to advantage. The large difference— 100-150dB— between transmitted and received powers precludes the use of a single telescope with some combination of optical circulators (40-60dB isolation at best) and polarization (limited by the polarization extinction ratio of PM fibers to 20-30dB at best). The use of single mode PM optical fiber in the transceiver, while ideal for providing good heterodyne mode and polarization matching as well as ease of alignment, presents additional difficulties. Co-axial placement of the transmit and receive apertures gives desirable beam-alignment geometries. However, because single mode fibers are so étendue-limited (10 μ m MFD with 0.1NA), central-obscurator structures significantly block the signal into a fiber placed at the focus of a collimated receive telescope from targets at a finite distance.³ This is seen in the short-range drop-off in the curves of Figure 5.

Our current design, shown schematically in Figure 4, is a simple compromise consisting of a fast (F/1) reflector-receiver with a 5cm primary, and a co-axial and centrally mounted transmit collimator using F/2 refractive optics, with a 15mm diameter beam waist. Figure 5 shows an analysis carried out using the ASAP software package. The model takes into account the actual telescope geometry and all obscurations. A primary Gaussian source at the fiber input of the collimator is propagated to a target to define an illuminated spot. The spot is then transformed to a secondary Lambertian source which is propagated to the receive telescope, where coupling into a fiber at the focus is calculated. This model therefore captures the range-dependent aspects of the geometry, while target reflectivity, free-space attenuation, and fiber misalignment are separately budgeted. As seen from the solid curve in Figure 5, the received signal from the central collima-

³An off-axis reflector design does not escape this— the zone of problematic obscurator translates from the clear-aperture to the optical axis.

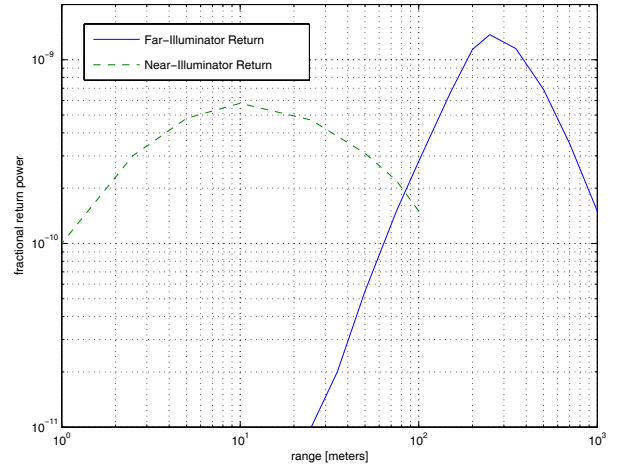


Figure 5: Return signal analysis from a geometric ASAP model. The fractional fiber-coupled return power from Lambertian-spots generated by both collimators is plotted as functions of range, showing both aperture-limited and obscurator-limited regimes.

tor falls into aperture-limited $1/R^2$ behavior past about 500m, but it also shows an unacceptable drop-off at short-ranges due to central-axis obscurator. A second, small collimator with a 1.6mm beam waist is therefore mounted at a hole drilled 15mm from the primary reflector optical axis to provide overlapping short-range coverage, extending it to within 1m.

This analysis was performed without regard to coherence effects, which will further limit the coupling into the fiber. The theoretical limit is 0.42 [3]; we plan for less in reality.

5 Conclusion

A better velocimeter is a crying need for EDL-TDC, and MCVA is our attempt to meet that need by applying some state-of-the-art photonics components to a sensor that will prove enabling for all near-future lunar and planetary surface missions.

References

- [1] L. Johnson and C. Cox. Serrodyne optical frequency translation with high sideband suppression. *Journal of Lightwave Technology*, 6(1):109–112, Jan 1988.
- [2] N. Takeuchi, N. Sugimoto, H. Baba, and K. Sakurai. Random modulation CW LIDAR. *Applied Optics*, 22:1382–1386, 1983.
- [3] P. Winzer and W. Leeb. Fiber coupling efficiency for random light and its application to LIDAR. *Optics Letters*, 23(13):986–988, 1998.